J Solid State Electrochem (2007) 11: 291–295
DOI 10.1007/s10008-006-0106-2

ORIGINAL PAPER

Aparna Banerjee · R. Prasad · V. Venugopal

Thermodynamic properties of the ternary oxides in the Eu–Ru–O system by using solid-state electrochemical cells

Received: 23 January 2006 / Revised: 25 January 2006 / Accepted: 27 January 2006 / Published online: 12 April 2006

Abstract The Gibbs free energies of formation of Eu_3RuO_7(s) and $Eu_2Ru_2O_7$(s) have been determined using solid-state electrochemical technique employing oxide ion conducting electrolyte. The reversible electromotive force (e.m.f.) of the following solid-state electrochemical cells have been measured:

$$\mathrm{Cell(I)}: (-)\mathrm{Pt}/\{Eu_3RuO_7(s) + Eu_2O_3(s) + Ru(s)\} \; //\mathrm{CSZ}//O_2(p(O_2) = 21.21\mathrm{kPa})/\mathrm{Pt}(+)$$

$$\mathrm{Cell(II)}: (-)\mathrm{Pt}/\{Eu_3RuO_7(s) + Eu_2Ru_2O_7(s) + Ru(s)\} \; //\mathrm{CSZ}//O_2(p(O_2) = 21.21\mathrm{kPa})/\mathrm{Pt}(+)$$

The Gibbs free energies of formation of Eu_3RuO_7(s) and $Eu_2Ru_2O_7$(s) from elements in their standard state, calculated by the least squares regression analysis of the data obtained in the present study, can be given, respectively, by:

$$\{\Delta_f G^o(Eu_3RuO_7, s)/(\mathrm{kJ \cdot mol^{-1}}) \pm 2.5) = -2,785.2 + 0.567 \cdot (T/\mathrm{K}); (922.5 \leq T/\mathrm{K} \leq 1194.9).$$

$$\{\Delta_f G^o(Eu_3Ru_2O_7, s)/(\mathrm{kJ \cdot mol^{-1}}) \pm 2.9) = -2,225.6 + 0.579 \cdot (T/\mathrm{K}); (995.3 \leq T/\mathrm{K} \leq 1260.6).$$

The uncertainty estimates for $\Delta_f G^o(T)$ include the standard deviation in e.m.f. and uncertainty in the data taken from the literature.

A. Banerjee (✉) · R. Prasad · V. Venugopal
Fuel Chemistry Division, Bhabha Atomic Research Centre,
Mumbai 400 085, India
e-mail: aparnab@apsara.barc.ernet.in
Tel.: +91-22-25590648
Fax: +91-22-25505151
e-mail: prasadr@apsara.barc.ernet.in
Fax: +91-22-25505345

Keywords System Eu–Ru–O · Europium ruthenates · Solid-state electrochemical technique · Gibbs free energy of formation

Introduction

A plethora of research has been initiated in recent years towards understanding the physical properties of 4d and 5d transition metal oxides, which show a variety of magnetic and transport transitions indicative of highly correlated electronic interactions and strong spin charge coupling [1]. There appears to be relatively few examples of oxides with both 4d transition metals and rare-earth constituents [2]. Most of these studies have been largely limited to pyrochlore systems such as $Ln_2Ru_2O_7$(s), where Ln is a rare earth element. Systematic studies on the thermodynamic properties of the compounds in the ternary system, Eu–Ru–O were carried out.

The Eu–Ru–O system investigated in this study comprises of two binary oxides: Eu_3RuO_7(s) and $Eu_2Ru_2O_7$(s). Eu_3RuO_7(s) was indexed on an orthorhombic unit cell (space group Cmcm) [3]. Physical properties such as magnetization, electrical resistivity and heat capacity of the ternary oxide were investigated by Harada et al. [4]. It was found to have nonmetallic electrical resistivity. Harada et al. [5] also found two transitions in Eu_3RuO_7(s) one at T=22.5 K due to a λ type second order transition and the other at 280 K due to a first order transition. The results indicate that the transition is a structural phase transition. Eu_3RuO_7(s) shows an antiferromagnetic transition due to Ru^{+5}ions at T_N=22.5 K, in accordance with the specific heat data.

In the pyrochlore oxide, $A_2^{+3}B_2^{+4}O_7^{-2}$ when both the A and B sites are occupied by magnetic ions, these compounds show very interesting magnetic features, caused by the coupled magnetic interactions between the 4f electrons of rare-earths and those between the d and g electrons [6, 7]. The ruthenium pyrochlores have been studied for their conductivity [8, 9] and catalytic activity

[10, 11]. The pyrochlore $Eu_2Ru_2O_7$(s) can be considered as an ordered defective fluorite (space group Fd3m). Magnetic properties for $Eu_2Ru_2O_7$(s) were measured by Taira et al. [2]. $Eu_2Ru_2O_7$(s) shows magnetic transition at T=120 K. Specific heat and susceptibility studies on $Eu_2Ru_2O_7$(s) were also carried out by Taira et al. [12]. $Eu_2Ru_2O_7$(s) shows a specific heat anomaly at 118 K.

Crystal structure, magnetic and electrical properties of the oxides have been thoroughly investigated by many researchers. However, thermodynamic properties of these oxides need investigation. Quantitative information on the thermodynamic properties of these compounds is useful for assessing the interaction of platinum group metals with ceramic compounds containing rare-earth oxides under different environments. The information is also important for the design of processes for the recovery of rare-earth and precious metals from scrap. In this study, based on the phase relations between the oxides, solid-state cells were designed to measure the Gibbs free energies of formation of the ternary oxides. The Gibbs free energies of formation of Eu_3RuO_7(s) and $Eu_2Ru_2O_7$(s) were determined by an oxide electrochemical cell using 0.15 mole fraction calcia stabilized zirconia (CSZ) solid electrolyte, in the temperature range from 922.5 to 1,194.9 K and from 995.3 to 1,260.6 K, respectively.

Materials and methods

Materials

Eu_3RuO_7(s) was synthesized from stoichiometric proportions of preheated Eu_2O_3(s) (0.9985 mass fraction, Leico Industries) and RuO_2(s) (0.997 mass fraction, Prabhat Chemicals, India). The oxides were intimately ground and the mixture was then pelletized. The pellet was subjected to a pressure of 50 MPa and then fired in air at T=1,273 K for several hours with repeated grindings. The pellet was reground and repelletized and heated in air several times to ensure homogeneity. The formation of the compound was confirmed by X-ray diffractometry. $Eu_2Ru_2O_7$(s) was prepared similarly by mixing and then pelletizing stoichiometric proportions of the respective oxides. The pellets were then sealed in an evacuated quartz ampoule and heated to T=1,423 K for several hours. The values of the interplanar d spacing obtained for Eu_3RuO_7(s) and $Eu_2Ru_2O_7$(s) recorded on Powder Diffractometer using $Cu-K_\alpha$ radiation is in good agreement with those reported in JCPDS file number #39-1028 [3] and #28-422 [13], respectively. Repeated attempts to synthesize Eu_2RuO_5(s), like RE_2RuO_5(s) (RE=Nd, Sm, Eu, Gd, Tb) type of materials failed as each time samples contained substantial second phases of $Eu_2Ru_2O_7$(s) [14, 15, 16].

Phase mixtures of {Eu_3RuO_7(s)+Eu_2O_3(s)+Ru(s)} and {Eu_3RuO_7(s)+$Eu_2Ru_2O_7$(s)+Ru(s)} in the appropriate molar ratios were pelletized into pellets of dimension 7 mm diameter and 3 mm thickness using a tungsten carbide die at a pressure of 100 MPa. The pellets were sintered in purified argon gas atmosphere at T=1,000 K for several hours. The sintered pellets were reexamined by X-ray diffraction and the phase compositions were found to be unchanged after sintering. These pellets were then used for e.m.f. measurements.

The oxide cell assembly

A double compartment cell assembly was used for e.m.f. measurements. The inner compartment was separated from the outer compartment by the use of an electrolyte tube. The electrolyte tube used was 0.15 mole fraction CSZ tube with one end closed and flat. The tube separated the gaseous environments over the two electrodes. The dimensions of the CSZ tube used were: 13 mm, outer diameter; 9 mm, inner diameter and 380 mm in length and was supplied by Nikatto, Japan. It was reported by Pratt [17] that the lower limit of oxygen partial pressures for purely ionic conduction of CSZ electrolyte is about 10^{-20} Pa at 1,000 K and 10^{-13} Pa at 1,273 K. Detailed experimental set up was described in an earlier publication [18]. An inert environment was maintained over the solid electrodes throughout the experiment by passing separate streams of purified argon gas. The argon gas was purified by passing it through towers containing the reduced form of BASF (Aktiengesellschaft, D-6700 Ludwigshafen, Germany) catalyst, molecular sieves, magnesium perchlorate, and hot uranium metal at 550 K. A Faraday cage made from stainless steel was placed between the furnace and cell assembly. The cage was grounded to minimize induced e.m.f. on the cell leads. A calibrated chromel–alumel thermocouple located in the vicinity of the pellets was used to monitor the cell temperature. The furnace temperature was controlled at ±1 K. Cell e.m.f. was measured by a Kiethley 614 electrometer (impedance >10^{14} Ω). Measurements were taken when the value of e.m.f. was steady for about 2–3 h using the high impedance electrometer. Voltages were reproducible in subsequent heating cycles. The following cell configurations were employed in the present study:

$$\mathrm{Cell(I)}: (-)\mathrm{Pt}/\{\mathrm{Eu_3RuO_7(s)} + \mathrm{Eu_2O_3(s)} + \mathrm{Ru(s)}\} \; //\mathrm{CSZ}//\mathrm{O_2(p(O_2) = 21.21kPa)/Pt}(+)$$

$$\mathrm{Cell(II)}: (-)\mathrm{Pt}/\{\mathrm{Eu_3RuO_7(s)} + \mathrm{Eu_2Ru_2O_7(s)} + \mathrm{Ru(s)}\} \; //\mathrm{CSZ}//\mathrm{O_2(p(O_2) = 21.21kPa)Pt}(+)$$

The reversibility of the solid-state electrochemical cells was checked by microcoulometric titration in both directions. A small quantity of current was passed through the cell in either direction. After the removal of the applied current, the cell e.m.f. returned to its original value. The e.m.f. of the cells were also found to be independent of flow rate of the inert gas passing over the electrodes. The X-ray diffraction pattern of the sample pellet after electrochemical measurements did not reveal any interaction between the equilibrium phases.

Results and discussion

Solid-state electrochemical measurements using oxide cell

E.m.f. of the solid state oxide electrochemical cell is related to the partial pressure of oxygen at the two electrodes and is given by the relation:

$$E = (RT/nF) \cdot \int_{p'(O_2)}^{p''(O_2)} t(O^{2-}) \cdot d \ln p(O_2) \quad (1)$$

E, is the measured e.m.f. of the cell in volts, R=8.3144 J K^{-1} $mol^{-1}$and is the universal gas constant, n is the number of electrons participating in the electrode reaction, F=96,486.4 C mol^{-1} is the Faraday constant, T is the absolute temperature, $t(O^{2-})$ is the effective transference number of O^{2-} ion for the solid electrolyte combination and $p'(O_2)$ and $p''(O_2)$ are the equilibrium oxygen partial pressures at the positive and negative electrodes, respectively. The transport number of oxygen ion in the present electrolyte cell arrangement is nearly unity ($t(O^{2-})$>0.99) at the oxygen pressures and temperatures covered in this study. Hence, the e.m.f. of the cell is directly proportional to the logarithm of the ratio of partial pressures of oxygen at the electrodes.

$\Delta_f G^o$ (T) of Eu_3RuO_7(s)

The reversible e.m.f.s of cell (I) measured as a function of temperature are listed in Table 1. The half-cell reactions at the cathode and the anode for cell (I) can be given by:

$$5/2\ O_2\,(g) + 10e^- = 5O^{2-}, \quad (\text{at the cathode}) \quad (2)$$

and,

$$3Eu_2O_3(s) + 2Ru(s) + 5/2\ O_2(g) = 2Eu_3RuO_7(s) + 10e^-, \quad (\text{at the anode}) \quad (3)$$

The overall cell reaction can be represented by:

$$3Eu_2O_3(s) + 2\,Ru(s) + 5/2\ O_2(g) = 2Eu_3RuO_7(s), \quad (4)$$

The least squared regression analysis of the e.m.f.s gives:

$$E/V(\pm 0.00313) = 0.6679 - 2.958 \cdot 10^{-4} \cdot (T/K); \quad (922.5 \le T/K \le 1,194.9). \quad (5)$$

The uncertainties quoted are the standard deviation in e.m.f. The $\Delta_r G^o(T)$ for the reaction given in Eq. 4 involves the transfer of ten electrons, and hence, from Nernst equation we get:

$$\Delta_r G^o(T) = -10FE = 2\Delta_f G^o\{Eu_3RuO_7(s)\} - 3\Delta_f G^o\{Eu_2O_3(s)\} - 5/2\ RT \ln p(O_2) \quad (6)$$

The value of $\Delta_f G^o(Eu_3RuO_7, s)$ has been obtained by combining Eq. 5 and $\Delta_f G^o$of (Eu_2O_3, s) from the literature [19].

$$\{\Delta_f G^o(Eu_3RuO_7, s)/(kJmol^{-1}) \pm 2.5\} = -2,785.2 + 0.567 \cdot (T/K). \quad (7)$$

The intercept and the slope of the above least square fit corresponds to the enthalpy of formation $\Delta_f H^o(T_{av.})$ and the entropy of formation $\Delta_f S^o(T_{av.})$, respectively, at T_{av}=1,058.7 K.

Table 1 The reversible e.m.f.s of the cell: (−)Pt/{Eu_3RuO_7(s) +Eu_2O_3(s)+Ru(s)}//CSZ//O_2($p(O_2)$=21.21 kPa)/Pt(+)

T/K	E/V	T/K	E/V
922.5	0.3930	1,081.9	0.3476
936.1	0.3900	1,128.2	0.3337
952.2	0.3832	1,140.8	0.3300
971.2	0.3786	1,173.1	0.3202
1,021.8	0.3720	1,194.9	0.3112
1,042.2	0.3637		
1,056.9	0.3586		

Table 2 The reversible e.m.f.s of the cell: (−)Pt/{Eu_3RuO_7(s) +$Eu_2Ru_2O_7$(s)+Ru(s)}//CSZ//O_2($p(O_2)$=21.21 kPa)/Pt(+)

T/K	E/V	T/K	E/V
995.3	0.4127	1,190.6	0.3137
1,020.0	0.4012	1,208.3	0.3090
1,034.6	0.3870	1,220.1	0.3028
1,067.1	0.3767	1,225.3	0.2996
1,077.6	0.3716	1,238.9	0.2932
1,090.2	0.3622	1,245.8	0.2909
1,109.9	0.3475	1,250.8	0.2884
1,137.6	0.3355	1,260.6	0.2800
1,160.8	0.3245		

$\Delta_f G^o\ (T)$ of $Eu_2Ru_2O_7(s)$

The reversible e.m.f.s of cell (II) measured as a function of temperature are listed in Table 2. The half-cell reactions at the cathode and the anode for cell (II) can be given by:

$$7/2\ O_2(g) + 14e^- = 7O^{2-}, (\text{at the cathode}) \quad (8)$$

and,

$$2Eu_3RuO_7(s) + 4Ru(s) + 7O^{2-} = 3Eu_2Ru_2O_7(s) + 14e^-, (\text{at the anode}) \quad (9)$$

The overall cell reaction can be represented by:

$$2Eu_3RuO_7(s) + 4Ru(s) + 7/2O_2(g) = 3Eu_2Ru_2O_7(s), \quad (10)$$

The least square regression analysis of the e.m.f.s gives:

$$E/V(\pm 0.00335) = 0.8879 - 4.811 \cdot 10^{-4} \cdot (T/\mathrm{K}); \quad (995.3 \le T/\mathrm{K} \le 1260.6). \quad (11)$$

The uncertainties quoted are the standard deviation in e.m.f. The $\Delta_r G^o(T)$ for the reaction given in Eq. 10 involves the transfer of 14 electrons.

$$\Delta_r G^o(T) = 3\Delta_f G^o\{Eu_2Ru_2O_7(s)\} - 2\Delta_f G^o\{Eu_3RuO_7(s)\} - 7/2\ RT\ \ln p(O_2). \quad (12)$$

$\Delta_f G^o(Eu_2Ru_2O_7, s)$ values have been obtained from Eqs 7 and 11.

$$\left\{\Delta_f G^o(Eu_2Ru_2O_7, s)/\left(\mathrm{kJ\,mol^{-1}}\right) \pm 2.9\right\} = -2,256.6 + 0.579 \cdot (T/\mathrm{K}). \quad (13)$$

The intercept and the slope of the above least squares fitted line corresponds to the enthalpy of formation $\Delta_f H^o(T_{av.})$ and the entropy of formation $\Delta_f S^o(T_{av.})$, respectively, at T_{av}=1,127.7 K.

Oxygen potential diagram

In ternary systems containing a volatile component such as oxygen, it is useful to visualize phase relations as a function of the chemical potential or partial pressure of the volatile species. In an isothermal oxygen potential diagram, the phase relations are represented as a function of partial pressure of oxygen. The oxygen potential diagram for the system Eu–Ru–O at T=1,250 K, computed from the results of this study, is shown in Fig. 1. The composition variable is the cationic fraction $\eta_{Ru}/(\eta_{Ru}+\eta_{Eu})$ where $\eta_i$represents moles of component i. Oxygen is not included in the composition parameter. The diagram provides useful information on the oxygen potential range for the stability of various phases. The diagram is complementary to the conventional Gibbs triangle representation of phase relations in ternary systems, where the composition of each phase can be unambiguously displayed. All the topological rules of construction for conventional binary temperature-composition phase diagrams are applicable to the oxygen potential diagram shown in Fig. 1. Though EuO (s) and Eu_3O_4(s) exist at T=1,250 K, their oxygen potentials are very low and hence, does not effect the phase field under consideration and are not shown in the oxygen potential diagram [20]. When three condensed phases coexist at equilibrium in a ternary system such as Eu–Ru–O the system is bivariant; at a fixed temperature and total pressure, three condensed phases can co-exist only at a unique partial pressure of oxygen. Therefore, horizontal lines on the diagram represent three phase equilibria. The equilibria at very low oxygen potentials between alloys and Eu_2O_3(s) are not shown in Fig. 1, as thermodynamic data for intermetallics required for the calculations are not available. These low oxygen potentials cannot be measured easily as they are well below the ionic conduction domain of oxide solid electrolytes. Similar

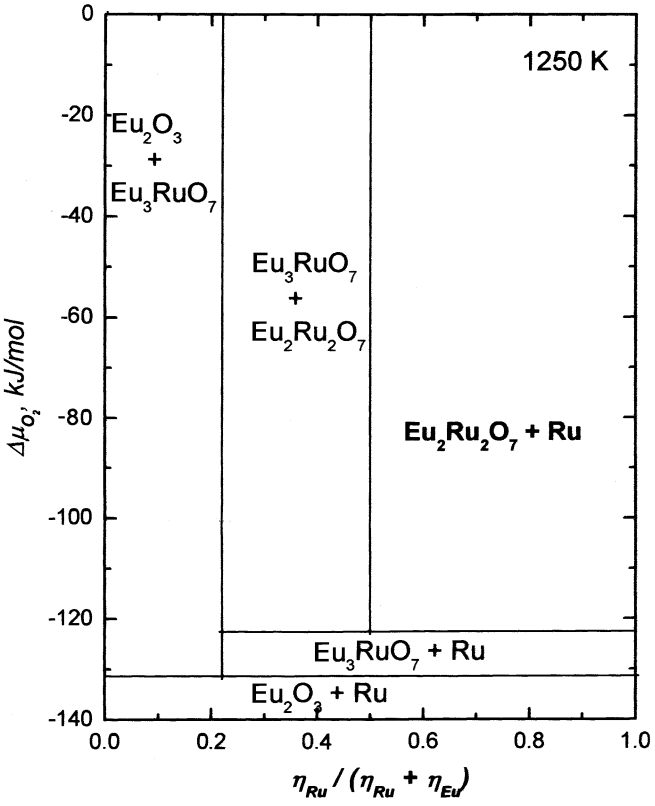

Fig. 1 Oxygen potential diagram of the Eu–Ru–O system at T=1,250 K

diagram at other temperatures can be readily computed from the thermodynamic data. Phase relations can also be computed as a function of temperature at constant oxygen partial pressures.

Conclusion

Ternary oxides in the Eu–Ru–O system have been prepared by the solid-state reaction route and characterized by X-ray diffraction analysis. The Gibbs free energies of formation of the ternary compounds were obtained by using solid state electrochemical oxide cells. The Gibbs free energies of formation of Eu_3RuO_7(s) and $Eu_2Ru_2O_7$(s) from elements in their standard state are: $\{\Delta_f G^o$ (Eu_3RuO_7, s)/(kJ mol^{-1})±2.5$\}$=−2,785.2+0.567·(T/K) and $\{\Delta_f G^o$($Eu_2Ru_2O_7$, s)/(kJ mol^{1})±2.9$\}$=−2,256.6+0.579·(T/K), respectively. Isothermal oxygen potential diagram was computed for the Eu–Ru–O system at T=1,250 K.

Acknowledgement The authors are grateful to Dr. K. D. Singh Mudher for providing the X-ray diffraction analysis performed by his group.

References

1. Cao G, McCall S, Crow JE, Guertin RP (1997) Phys Rev Lett 78:1751
2. Taira N, Wakeshima M, Hinatsu Y (1999) J Phys: Condens Matter 11:6983
3. van Berkel FPF, Ijdo DJW (1986) Mater Res Bull 21:1103
4. Harada D, Hinatsu Y (2001) J Phys: Condens Matter 13:10825
5. Harada D, Hinatsu Y (2001) J Solid State Chem 158:245
6. Taira N, Wakeshima M, Hinatsu Y (1999) J Solid State Chem 144:216
7. Taira N, Wakeshima M, Hinatsu Y, Tobo A, Ohoyama K (2003) J Solid State Chem 176:165
8. Pike GE, Seager CH (1977) J Appl Phys 48:5152
9. Carcia PF, Ferreti A, Suna A (1982) J Appl Phys 53:5282
10. Horowitz HS, Longo JM, Horowitz HH (1983) J Electrochem Soc 130:1851
11. Egdell RG, Goodenough JB, Hamnett A, Naish CC (1983) J Chem Soc Faraday Trans 79:893
12. Taira N, Wakeshima M, Hinatsu Y (2000) J Solid State Chem 152:441
13. Smith, McCarthy (1975) Penn State Univ., Univ. Park, Pennsylvania, U.S.A., JCPDS Grant-in-Aid Report
14. Cao G, McCall S, Zhou ZX, Alexander CS, Crow JE, Guertin RP, Mielke CH (2001) Phys Rev B 63:144427
15. Cao G, McCall S, Zhou ZX, Alexander CS, Crow JE, Guertin RP (2001) J Magn Magn Mater 226:218
16. Guertin RP, McCall S (2001) Inter J Mod Phys B 16:3317
17. Pratt JN (1990) Metall Trans A 21A:1223
18. Singh Z, Dash S, Prasad R, Sood DD (1994) J Alloys Compd 215:303
19. Barin I (1995) *Thermochemical Data of Pure Substances*, vols. I and II, third edn. VCH, New York
20. Pankratz LB (1982) *Thermodynamic Properties of Elements and Oxides*, Bulletin 672. United States Bureau of Mines